



Journal of Advanced Research in Fluid Mechanics and Thermal Sciences

Journal homepage:
https://semarakilmu.com.my/journals/index.php/fluid_mechanics_thermal_sciences/index
ISSN: 2289-7879



A Simulation Method of 2D Steady Scalar Convection-Diffusion Flow on an Exponentially Graded Mesh

Aslam Abdullah^{1,*}

¹ Department of Aeronautical Engineering, Faculty of Mechanical and Manufacturing Engineering, Universiti Tun Hussein Onn Malaysia, 86400 Parit Raja, Batu Pahat, Johor, Malaysia

ARTICLE INFO

Article history:

Received 8 December 2022
Received in revised form 19 March 2023
Accepted 25 March 2023
Available online 13 April 2023

Keywords:

Convection-diffusion; exponentially graded mesh; Peclet-mesh number relation

ABSTRACT

Owing to its fundamental nature, convection-diffusion flows are researched in a number of engineering, scientific, and aeronautical applications. The right meshing approaches are necessary for convection-diffusion simulations. Major meshes in computational fluid dynamics that are used to find the solutions to discretized governing equations include uniform, piecewise-uniform, graded, and hybrid meshes. Unintentionally applying the meshes might lead to poor solutions including numerical oscillations, over- or under-predictions, and lengthy computing time. Accentuating the effectiveness of exponentially graded mesh finite-difference scheme, this paper takes the simulation of a 2D steady scalar convection-diffusion into account. The problem was solved by assigning certain mesh expansion factor to the mesh according to Peclet number. The factor was determined based on its previously derived logarithmically linear relationship with low Peclet number. Based on the values of Peclet number and the source, eight groups of test cases are presented in this paper. It was found that given a Peclet and a mesh number, simulation error percentage was surprisingly constant regardless the source values. The rates of convergence for the scheme, however, were comparable with respect to source values. Uniform convergence rate was also found to be achievable in all test cases corresponding to Peclet number of interests. This work successfully assessed the validity range of the generalized logarithmically linear model between exponentially graded mesh expansion factor and Peclet number for the simulation.

1. Introduction

1.1 Graded Mesh

Extensive discussions on graded mesh have been motivated by other structured meshes as uniform and Shishkin meshes with the principal intention of avoiding uneconomical mesh refinement [1-5]. Early researches gave general attention on using the graded mesh by, for instance, choosing the right mesh grading for piecewise polynomial interpolation and for approximating solutions to two-point boundary value problems using finite difference or finite element techniques [1]. Later studies showed further variations of the mesh such as an exponentially graded mesh, and their

* Corresponding author.

E-mail address: aslam@uthm.edu.my

<https://doi.org/10.37934/arfmts.105.1.7689>

advantages against Shishkin mesh in solving convection-diffusion problems [2,3]. More advanced cases included the application of highly graded unstructured mesh, and more complete classification of the mesh into simply, exponentially, and aggressively graded meshes [4,5].

Intuitively, one may grade the mesh so that the domain is effectively spread over the change in, say, scalar concentration C . While many problems may find this grading function to be helpful and produce decent numerical results, there are pathological circumstances where it will collapse or cause issues. For instance, it is clear that the approach will not work if mesh number N is odd and C is symmetric in x where it has a single maximum. However, this example demonstrates the concept of a grading function in a straightforward, natural setting. From the perspective of piecewise-polynomial interpolation, the concept of an optimal mesh and grading function in a given norm or seminorm was investigated by Carey and Dinh [1]. An analysis of the optimality of the mesh and function led to the formulation of an adaptive mesh redistribution algorithm for boundary-value problems in 1D. Additionally, it was demonstrated how minor perturbations are impacted by the grading function. The findings from the graded interpolation problem and the adaptive technique for the boundary-value problem have great correlation, especially for the finer meshes. A set of grading functions and a related algorithm were developed in response to the challenge of mesh redistribution to provide an optimal piecewise-polynomial interpolant in a given norm or seminorm. This study and algorithm were then expanded to address the issue of choosing a graded mesh for two-point boundary-value problems that can be approximated using finite difference or finite element [1].

Gartland [2] presented a family of finite-difference techniques based on an exponentially graded mesh and local polynomial basis functions. These schemes were designed to have a consistent and arbitrarily high order of convergence. By employing additional local evaluations of the coefficient functions and source term in the two-point boundary value issue, the high order is attained. Both researchers focused on challenges related to mesh grading and its effects on finite-difference techniques in particular. Their biggest obstacle to stability seemed to be the requirement to "upwind" enough when moving across the extremely constrained transition zones between "inner" and "outer" mesh spacings. With the intention of laying out a process for the construction of the schemes that satisfy the stability theorems and have an order of convergence that is uniform in the diffusivity ε and can be made as high as desired, the construction of polynomial-based, compact finite-difference discretizations of their problem on a specific graded mesh was taken into consideration. The computational domain was fundamentally separated into three areas by the graded mesh: the uniformly wide outside region, the transition region, and the graded interior region. The spacing must be approximately consistent in areas where the singular perturbation parameter (i.e., sufficiently small ε) was tiny in comparison to the local mesh spacing. It was established that the schemes had high uniform stability [2].

By employing a properly graded mesh that corresponds to three boundary layers, it is possible to get optimal error order estimates that are valid uniformly up to a logarithmic factor in the sufficiently small ε . After establishing a consistent division at the outset, Durán and Lombardi [3] began the grading process. A few numerical examples demonstrated the method's successful operation. In particular, the approach accurately approximated the conventional piecewise bilinear finite element solution of the convection-diffusion equations. The graded mesh method appeared to be more reliable in that changes in the parameters defining the mesh have less of an impact on the numerical outcomes. Following an error analysis, a graded mesh was created that successfully accommodated both small and large perturbation parameters. Comparatively, the well-known Shishkin mesh's findings are significantly influenced by the parameter specifying the moment at which the mesh's size changes. If this parameter is somewhat off from its ideal setting, oscillations in the numerical solution may be seen. Additionally, the Shishkin mesh no longer functions properly for greater values

of the singular perturbation parameter. It was built for a certain value of the parameter. As a result, the graded mesh appears to be a compelling alternative to the Shishkin mesh, which likewise offers optimal order for situations of this nature [3].

A more complex mesh includes highly graded unstructured meshes discussed by Nochetto [4]. The analysis carried over regardless of convexity and accounted even for slit domains. Nochetto [4] indicated the piecewise linear finite element solution defined over the mesh made of triangles. The mesh was unstructured in the sense that the triangles at comparable distance to a singularity were not necessarily of comparable size.

When used in conjunction with techniques like non-standard integral equations and specialised interpolatory quadrature methods, for example, graded mesh can accelerate convergence even more. Mesh around solitary boundary points may be improved using a variety of techniques. In contrast to an aggressively graded mesh that was developed using a more sophisticated approach, aiming for fewer subdivisions to obtain a given resolution, a simple graded mesh was refined by Helsing and Ojala [5] using binary subdivision. They used a multilayer preconditioning approach called recursive compressed inverse preconditioning, which was based on a coarse mesh and a hierarchy of meshes on a simply graded mesh. The end goal was a top-level equation that was properly conditioned. The simply graded mesh needed no grading exponent and less specialised interpolatory quadrature. This was shown to significantly enhance performance and resuscitate integral equation formulations that would often be abandoned owing to heavy refining requirements [5].

1.2 Mesh Independent Issues and Code Errors

The CFD computation for the coarse mesh is clearly not yet mesh independent and may cause significant erroneous results. The reliability of the numerical solution to a specific problem that is posed by the mesh and boundary conditions utilised is often examined by CFD mesh independence studies [6-8]. The solution profile for coarse and relatively finer mesh might apparently be the same even near the boundaries where it is especially important to have mesh independence. It would therefore be beneficial to increase the mesh resolution even further to resolve the slight discrepancy, usually by keep decreasing mesh width by half. While this may seem straightforward, a full mesh-independence study would require running a case with as high as hundreds of thousands to millions mesh points for complex flow analysis to capture the main features [8,9]. Efficient mesh adaptation can yield a coarser mesh where the mesh points may be reduced by approximately an order of magnitude. The particular adaptation procedure aims at providing higher mesh resolution in regions with high variable gradients. In addition, higher order schemes are used, and computations are performed in double precision to increase accuracy [8].

The CFD setup also affects the outcomes of mesh independence tests. They can differ amongst meshes of the same resolution, vary depending on the flow conditions or directions that are simulated, and between CFD solvers owing to variations in discretization schemes, turbulence models, etc. The list is endless [6,7].

Iteration and time-step convergence analysis for response variables (such as resistance coefficients, wetted surfaces, and dynamic trim angles) carried out using the primary error and uncertainty estimation methods are also included in an extended verification and validation study of CFD simulations, in addition to the mesh independence test. Typically, the mesh number has an inverse relationship with the number of iterations [10].

Ge and Zhang [11] offered an intriguing scenario in which they claimed that, when used to solve elliptic problems, the geometric multimesh method's mesh independent convergence rate is likely its best-known characteristic. When $\varepsilon = 10^{-3}$, the impact of mesh stretching on the convergence

dependency was examined. When the mesh was not stretched, it was discovered that a mesh independent convergence rate was achievable. The multimesh convergence rate with a stretched mesh depended on the mesh size. But what was intriguing about such a reliance was its very essence. The convergence rate increased when the mesh was improved with only a slight stretching. When the mesh was refined with a significant stretching, the convergence rate decreased [11].

Code errors, particularly runtime errors, are another challenge which needs to be overcome in order to run a numerical model. There are various methods to circumvent such errors. Because everything starts with a mesh it is paramount to overcome these errors by providing it with a friendly geometry that it can successfully mesh. Among the most common errors are an overflow error and a divide-by-zero error. Both are categorized as floating point exception (FPE) which is a result of computation returning either a NaN (not-a-number) or a stack overflow [11].

1.3 Convection-diffusion Model

The differential form of the generic scalar conservation equation in rectangular coordinates and tensor notation is [12]

$$\partial_t(\rho C) + \partial_{x_j}(\rho u_j C) = \partial_{x_j}(\varepsilon \partial_{x_j} C) + e_C \quad (1)$$

where t stands for time, ρ for density, C for a scalar quantity, x_j ($j = 1,2,3$) or (x, y, z) are the Cartesian coordinates, u_j or (u, v, w) are the Cartesian components of the velocity vector \mathbf{V} , ε is the diffusivity for the quantity C , and e_C represents source or sink of C . Finite difference method will be described in this paper for this generic conservation equation.

We solve the steady 2D scalar convection-diffusion equation with Dirichlet boundary conditions. The steady state equation with quadratic source term to be solved reads

$$\partial_x(\rho u C) = \partial_x(\varepsilon \partial_x C) - 4y^2 + 4y \quad (2)$$

with the boundary conditions $C = C_0$ at $x = 0$, $C = C_L$ at $x = L$, where L is the width and height of the domain as in Figure 1 to Figure 3. In this case, ordinary derivatives may replace the partial derivatives.

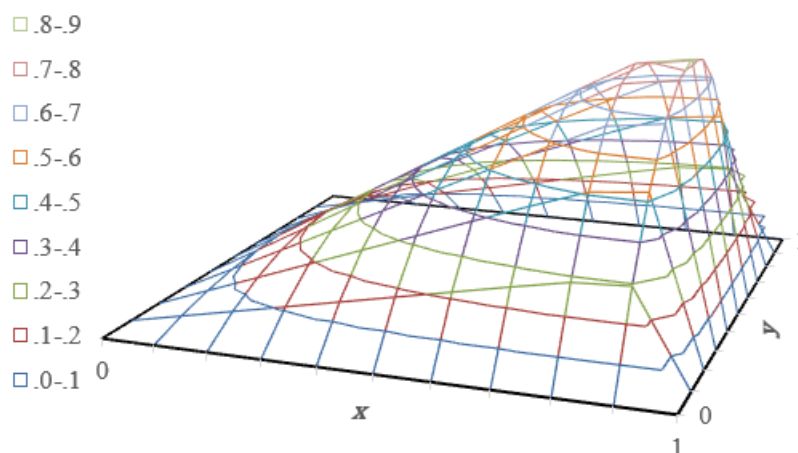


Fig. 1. Theory-based profile in a unit square domain when $Pe \gg 0$

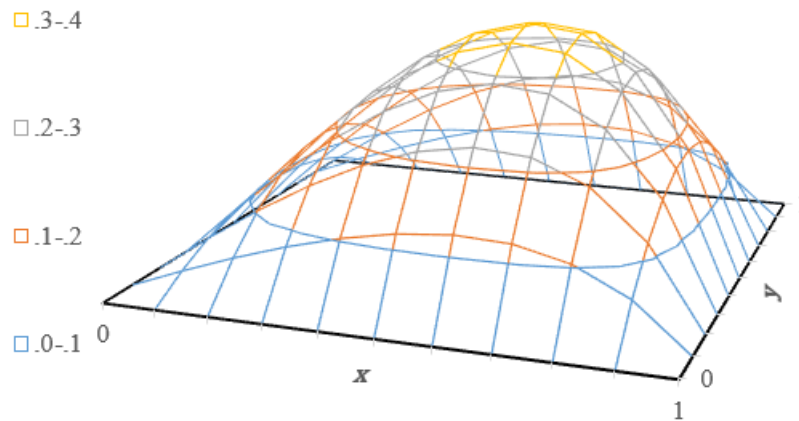


Fig. 2. Theory-based profile in a unit square domain when $Pe > 0$

If the density ρ and the velocity u are unity and $C_0 = C_L = 0$, the problem exact solution in a simple unit square domain $0 \leq x \leq 1$ and $0 \leq y \leq 1$ reads

$$C^{exact} = \epsilon c_1 e^{x/\epsilon} + e_c x + c_2 \quad (3)$$

where c_1 and c_2 are constants of integration, given by

$$c_1 = -\frac{e_c}{\epsilon e^{1/\epsilon} - \epsilon} \quad (4)$$

and

$$c_2 = -\epsilon c_1, \quad (5)$$

respectively. Note that u being unity represents the case where $u \geq 0$.

This problem physically represents a situation in which convection is balanced by diffusion and source in the streamwise direction. Numerical methods developed for Eq. (2) may be applied to the Navier-Stokes equations. This problem raises some of the issues worthy of attention.

When the velocity is small (i.e., $u \approx 0$) or diffusivity C is large, the Peclet number defined as

$$Pe = \frac{\rho u L}{\epsilon} \quad (6)$$

tends to zero and convection is negligible; the solution is then symmetric in x as shown in Figure 3. In the case of large Peclet number, C grows slowly with x and then suddenly drops to C_L over a short distance close to $x = L$, as previously illustrated in Figure 1 and Figure 2. The rapid change in the absolute gradient value provides a severe test of the simulation method.

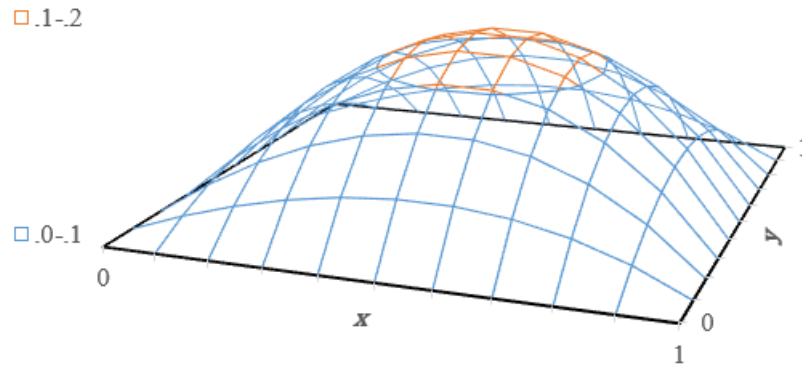


Fig. 3. Theory-based profile in a unit square domain when $Pe \approx 0$

In fluid mechanics, Eq. (1) is extended to represent some of the most fundamental phenomena which include the transport of heat, mass, and momentum [13,14]. It is extremely important to model and describe the phenomena in various engineering disciplines, aviation, meteorology, and physical sciences [13-25]. The mathematical framework for heat and mass transfer are of same kind, and basically encompassed by advection and diffusion effects. An initially discontinuous profile is propagated by diffusion and convection (or advection), the latter with a speed, in such general scalar transport equations [13,23,24]. These equations are frequently used in computational simulations, such as wake vortex simulation in aviation, petroleum reservoir simulation, and global weather prediction [19,20,26].

The motivation for this work is to accurately simulate the behaviour of scalar quantities such as temperature or chemical concentration in fluid flows. The simulation method proposed in this paper is based on an exponentially graded mesh and uses a finite difference scheme [27]. The use of the mesh is effective in solving convection-diffusion equations and allows for a more accurate representation of the flow behaviour near the boundary layers [27,28].

This paper builds on previous research in the field of CFD, including the works by Mohammadi [28], Shan [29] and Wu and Xu [30]. Thus, this work on 2D steady scalar convection-diffusion model and the use of logarithmically linear model between expansion factor r_e and Peclet number Pe for the corresponding simulation is a contribution to the field. Moreover, it has the potential to be applied to a wide range of engineering, ecological, and geophysical applications that involve the dispersal and mixing of scalar quantities in fluid flows [31].

Correct meshing approaches including graded mesh are essential for simulating fluids flow. Uncareful application of exponentially graded mesh might lead to poor solutions including numerical oscillations, over- or under-predictions, and lengthy computing time. This paper analyzes the effectiveness of exponentially graded mesh finite-difference scheme for simulating 2D steady scalar convection-diffusion flow. The aim is to assess the validity range of the generalized logarithmically linear model between expansion factor r_e and Peclet number Pe for the simulation.

2. Methodology

We discretized Eq. (2) using finite difference method which uses the three-point computational atom. The resulting algebraic equation at each internal node is

$$BC_{i-1} + DC_i + AC_{i+1} = e_p \quad (7)$$

where B, D, A are the first lower, main, and first upper diagonal elements of tridiagonal coefficient matrix, respectively [32]. All other elements are zero.

The diffusion term was discretized using central difference scheme (CDS) as commonly practiced. The outer derivative is thus given by

$$-[\partial_x(\epsilon\partial_x C)]_i \approx \frac{(\epsilon\partial_x C)_{i+\frac{1}{2}} - (\epsilon\partial_x C)_{i-\frac{1}{2}}}{\frac{1}{2}(x_{i-1} - x_{i+1})} \quad (8)$$

The inner derivatives were approximated with CDS as

$$(\epsilon\partial_x C)_{i+\frac{1}{2}} \approx \epsilon \frac{C_{i+1} - C_i}{x_{i+1} - x_i} \quad (9)$$

$$-(\epsilon\partial_x C)_{i-\frac{1}{2}} \approx \epsilon \frac{C_i - C_{i-1}}{x_{i-1} - x_i} \quad (10)$$

The contributions of the diffusion term to the coefficients B, A, D in Eq. (7) are

$$B^{diff} = \frac{2\epsilon}{(x_{i+1} - x_{i-1})(x_{i-1} - x_i)}, \quad (11)$$

$$A^{diff} = \frac{2\epsilon}{(x_{i+1} - x_{i-1})(x_i - x_{i+1})}, \quad (12)$$

and

$$D^{diff} = -(B^{diff} + A^{diff}), \quad (13)$$

respectively.

Similarly, the convection term was discretized using CDS which led to

$$[\partial_x(\rho u C)]_i \approx -\rho u \frac{C_{i+1} - C_{i-1}}{x_{i-1} - x_{i+1}} \quad (14)$$

The contributions of the convection term to the coefficients B, A, D in Eq. (7) are

$$B^{conv} = -\frac{\rho u}{x_{i+1} - x_{i-1}}, \quad (15)$$

$$A^{conv} = \frac{\rho u}{x_{i+1} - x_{i-1}}, \quad (16)$$

and

$$D^{conv} = -(B^{conv} + A^{conv}) = 0, \quad (17)$$

respectively.

Defining mesh point in the x -direction for $r_e = 1$;

$$x_1 = 0 \tag{18}$$

$$\Delta x = \frac{1}{N} \tag{19}$$

$$x_i = x_{i-1} + \Delta x \tag{20}$$

where $i = 2, 3, \dots, N$.

Defining mesh point in the x -direction for $r_e \neq 1$;

$$x_1 = 0 \tag{21}$$

$$(\Delta x)_1 = \frac{1-r_e}{1-r_e^N} \tag{22}$$

$$(\Delta x)_i = r_e (\Delta x)_{i-1} \tag{23}$$

where $i = 2, 3, \dots, N - 1$.

$$x_i = x_{i-1} + (\Delta x)_{i-1} \tag{24}$$

where $i = 2, 3, \dots, N$.

Defining mesh point in the y -direction;

$$y_1 = 0 \tag{25}$$

$$\Delta y = \frac{1}{N} \tag{26}$$

$$y_i = y_{i-1} + \Delta y \tag{27}$$

where $i = 2, 3, \dots, N$.

Exponentially graded mesh was only applied in x -coordinates along which the change in the mesh width Δx is exponential, while uniform mesh in y -coordinates. This was due to the derivatives in Eq. (2) were those with respect to x only, thus non-uniform mesh in y -coordinates was unnecessary. Both mesh number N and mesh expansion factor r_e affect mesh width (i.e., the distance between two neighboring computational atoms) Δx . The mesh shown in Figure 4 is stretched to a coarser mesh away from $x = 1$. In general, the mesh width on both coarse and fine part of mesh decreases when N increases and r_e is fixed. On the other hand, the mesh width on coarse part of mesh decreases, while that on fine part increases when r_e increases and N is fixed. For $r_e = 1$, mesh is identical to uniform mesh, where all neighboring computational atoms are equally spaced from one another for all N .

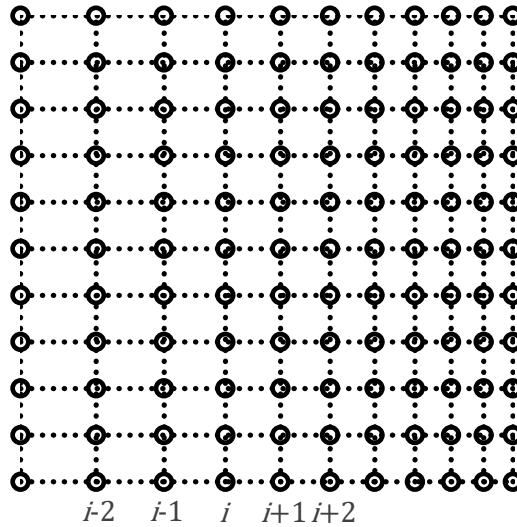


Fig. 4. Exponentially graded mesh in x with computational atoms

Over- and under-reduction of r_e would result in the overall profile of C is under-predicted and oscillates, respectively. Note that even for the small N (e.g., $N = 11$), computational atoms on the fine part of mesh are extremely densed for small r_e (e.g $r_e = .5$) such that they are not easily visually distinguishable. For $r_e \rightarrow 0$ and $r_e \rightarrow 1$, $(\Delta x)_{coarse} \rightarrow 1$ and $\Delta x \rightarrow 1/(N - 1)$, respectively, where $(\Delta x)_{coarse}$ is the mesh width on the coarse part. For $N \rightarrow 2$ and $N \rightarrow \infty$, $\Delta x \rightarrow 1$ and $\Delta x \rightarrow 0$, respectively.

In the prediction of convection-diffusion flow with quadratic source, the expansion factor r_e is logarithmically inversely proportional to the low Peclet number Pe [33];

$$r_e = m \lg Pe + b, \tag{28}$$

where

$$m = \frac{.5}{(\lg .03125)}, \tag{29}$$

and

$$b = 1. - (m \lg 3.125), \tag{30}$$

are curve slope and a constant, respectively. The relationship in Eq. (28) was initially used for $N = 11$ [33]. Here we generalize its use for $N \geq 11$. Note that our Pe of interests are those of 3.125, 6.25, 12.5, and 25.

For mesh independency tests one mesh with $N = 11$ was generated, and the numerical simulation (first level) was compared to that on a two times finer grid (second level), and so forth.

We defined the simulation error as

$$Err = \frac{\sum_i |c_i^{exact} - c_i|}{N}, \tag{31}$$

and the simulation error percentage

$$Err\% = \frac{Err \times N}{\sum_i C_i^{exact}} \times 100\%, \quad (32)$$

where $i = 1, 2, \dots, N$. The error ratio is given by

$$Erratio_m = \frac{Err_{(N-1)m-1}}{Err_{(N-1)m}}, \quad (33)$$

where $m = 2, 3, 4, \dots$, and the rate of convergence

$$p = \frac{Erratio_m}{2} \quad (34)$$

3. Results

The concentration of scalar C was calculated numerically and analytically in 2D over exponentially graded meshes for various values of N . The simulation error, Err , error percentage, $Err\%$, error ratio, $Erratio$, and rate of convergence, p , were also tabulated with respect to Peclet number, Pe , and N . The exact solutions were used as benchmarks for validation of the numerical simulations. The concentration at two specific locations, $y|_{e_p=0.64}$ and $y|_{e_p=1}$, represent the concentration when the source is relatively small and maximum, respectively.

Data in Table 1 and Table 2 when $Pe = 3.125$ represent those when $r_e = 1$ where the mesh is identical to uniform mesh. In the case of $Pe = 3.125$, the error is relatively higher when $e_p = 1$ in comparison to $e_p = 0.64$, with a maximum difference in error of 5.0×10^{-4} when $(N - 1) = 10$. The optimum mesh number of 640 corresponds to an error percentage of 0%. Despite the differences in error, the error percentage remains constant while the error ratio values are very similar for the same $(N - 1)$. The simulation error percentage has a maximum value of 0.616%, which corresponds to $(N - 1) = 10$.

Table 1
 Numerical errors when $Pe = 3.125, e_p = 0.64$

$N - 1$	Err	$Err\%$	$Erratio$	p
10	8.0×10^{-4}	0.616 %		
20	2.1×10^{-4}	0.153 %	3.8	1.9
40	5.4×10^{-5}	0.038 %	3.9	1.9
80	1.4×10^{-5}	0.010 %	3.9	1.9
160	3.5×10^{-6}	0.002 %	4.0	2.0
320	8.8×10^{-7}	0.001 %	4.0	2.0
640	2.4×10^{-7}	0.000 %	3.7	1.8

Table 2
 Numerical errors when $Pe = 3.125, e_p = 1$

$N - 1$	Err	$Err\%$	$Erratio$	p
10	1.3×10^{-3}	0.616 %		
20	3.3×10^{-4}	0.153 %	3.9	2.0
40	8.5×10^{-5}	0.038 %	3.9	1.9
80	2.2×10^{-5}	0.010 %	3.9	1.9
160	5.4×10^{-6}	0.002 %	4.1	2.0
320	1.4×10^{-6}	0.001 %	3.9	1.9
640	3.7×10^{-7}	0.000 %	3.8	1.9

Table 3 and Table 4 show that when $Pe = 6.25$, the error (Err) is substantially greater when $e_p = 1$ than when $e_p = 0.64$, with a maximum difference in error of 9.0×10^{-4} when $(N - 1) = 10$. When a uniform rate of convergence is attained (i.e., when $p = 1.0$), the optimal mesh number of 80 corresponds to an error percentage ($Err\%$) of 0.026%. Despite the differences in error, the error percentage remains constant while the error ratio ($Erratio$) values are very similar for the same $(N - 1)$. Note that $Err\%$ has a maximum value of 0.775%, which corresponds to $(N - 1) = 10$.

Table 3
 Numerical errors when $Pe = 6.25, e_p = 0.64$

$N - 1$	Err	$Err\%$	$Erratio$	p
10	1.6×10^{-3}	0.775 %		
20	2.6×10^{-4}	0.122 %	6.2	3.1
40	5.7×10^{-5}	0.031 %	4.6	2.3
80	2.8×10^{-5}	0.026 %	2.0	1.0
160	1.4×10^{-5}	0.026 %	2.0	1.0
320	7.1×10^{-6}	0.026 %	2.0	1.0

Table 4
 Numerical errors when $Pe = 6.25, e_p = 1$

$N - 1$	Err	$Err\%$	$Erratio$	p
10	2.5×10^{-3}	0.775 %		
20	4.1×10^{-4}	0.122 %	6.1	3.0
40	8.9×10^{-5}	0.031 %	4.6	2.3
80	4.3×10^{-5}	0.026 %	2.1	1.0
160	2.2×10^{-5}	0.026 %	2.0	1.0
320	1.1×10^{-5}	0.026 %	2.0	1.0

Table 5 and Table 6 show data corresponding to $Pe = 12.5$, where the error (Err) is comparatively higher when $e_p = 1$ in comparison to $e_p = 0.64$, with a maximum difference in error of 1.1×10^{-3} when $(N - 1) = 10$. When a uniform simulation error percentage is attained (i.e., when $Err\% = 0.132\%$), the optimal mesh number of 40 corresponds to a rate of convergence (p) of 1.1. Despite the differences in error, the error percentage ($Err\%$) remains constant while the error ratio ($Erratio$) values are very similar for the same $(N - 1)$. Obviously, the simulation error percentage has a maximum value of 0.763%, which corresponds to $(N - 1) = 10$.

Table 5
 Numerical errors when $Pe = 12.5, e_p = 0.64$

$N - 1$	Err	$Err\%$	$Erratio$	p
10	2.1×10^{-3}	0.763 %		
20	4.3×10^{-4}	0.178 %	4.9	2.4
40	1.9×10^{-4}	0.132 %	2.3	1.1
80	9.9×10^{-5}	0.132 %	1.9	1.0

Table 6
 Numerical errors when $Pe = 12.5, e_p = 1$

$N - 1$	Err	$Err\%$	$Erratio$	p
10	3.2×10^{-3}	0.763 %		
20	6.8×10^{-4}	0.178 %	4.7	2.4
40	3.0×10^{-4}	0.132 %	2.3	1.1
80	1.6×10^{-4}	0.132 %	1.9	0.9

Table 7 and Table 8 show the general scenario when $Pe = 25$, where the error (Err) is substantially greater when $e_p = 1$ than when $e_p = 0.64$, with a maximum difference in error of 1.2×10^{-3} when $(N - 1) = 10$. When a uniform rate of convergence is attained (i.e., when $p = 1.0$), the optimal mesh number of 40 corresponds to an error percentage ($Err\%$) of 0.256%. It is interesting to note that the simulation corresponding to $(N - 1) = 160$ was not achievable due to a code error (FPE). Despite the differences in error, the error percentage remains constant while the error ratio ($Erratio$) values are very similar for the same $(N - 1)$. It is worth noting that $Err\%$ has a maximum value of 0.684%, which corresponds to $(N - 1) = 10$.

Table 7

Numerical errors when $Pe = 25, e_p = 0.64$

$N - 1$	Err	$Err\%$	$Erratio$	p
10	2.1×10^{-3}	0.684 %		
20	6.2×10^{-4}	0.268 %	3.4	1.7
40	3.1×10^{-4}	0.256 %	2.0	1.0
80	1.6×10^{-4}	0.255 %	1.9	1.0

Table 8

Numerical errors when $Pe = 25, e_p = 1$

$N - 1$	Err	$Err\%$	$Erratio$	p
10	3.3×10^{-3}	0.684 %		
20	9.7×10^{-4}	0.268 %	3.4	1.7
40	4.9×10^{-4}	0.256 %	2.0	1.0
80	2.5×10^{-4}	0.255 %	2.0	1.0

It was observed that simulation error percentage ($Err\%$) remained constant regardless of the source values (e_p) for a given Peclet number and mesh number. The rates of convergence (p) were also found to be very similar with respect to e_p , indicating that there was no strong relationship between p and e_p . The difference between the error when $e_p = 0.64$ and $e_p = 1$ ($Err|_{e_p=0.64}$ and $Err|_{e_p=1}$) increases with Pe for a given $(N - 1)$, with the maximum difference occurring at $(N - 1) = 10$ in all cases of Pe . Optimal mesh numbers were successfully determined based on the convergence of $Err\%$ and the uniform rate of convergence p in all cases.

4. Conclusions

The analysis of the effectiveness of the exponentially graded mesh finite-difference scheme for simulating 2D steady scalar convection-diffusion flow has succeeded in assessing the validity range of the generalized logarithmically linear model between expansion factor r_e and Peclet number Pe . The results prove that the model which was initially used for $N = 11$ can be extended for $N \geq 11$ with respect to $Pe = 3.125, 6.25, 12.5, 25$ for increased solution accuracy and optimal mesh number.

The study involving higher Pe can be considered in order to increase the mesh robustness. Note that high Pe leads to floating-point error which necessitates more complex mesh. The problem might be handled by fundamentally separating computational domain into outside region, transition region, and graded interior region to determine whether the technique is compatible with the generalized logarithmically linear model.

Acknowledgement

This research was supported by Universiti Tun Hussein Onn Malaysia (UTHM) through Tier 1 (vot Q115).

References

- [1] Carey, Graham F., and Hung T. Dinh. "Grading functions and mesh redistribution." *SIAM Journal on Numerical Analysis* 22, no. 5 (1985): 1028-1040. <https://doi.org/10.1137/0722061>
- [2] Gartland, Eugene C. "Graded-mesh difference schemes for singularly perturbed two-point boundary value problems." *Mathematics of Computation* 51, no. 184 (1988): 631-657. <https://doi.org/10.1090/S0025-5718-1988-0935072-1>
- [3] Durán, Ricardo G., and Ariel L. Lombardi. "Finite element approximation of convection diffusion problems using graded meshes." *Applied Numerical Mathematics* 56, no. 10-11 (2006): 1314-1325. <https://doi.org/10.1016/j.apnum.2006.03.029>
- [4] Nochetto, Ricardo H. "Pointwise a posteriori error estimates for elliptic problems on highly graded meshes." *Mathematics of Computation* 64, no. 209 (1995): 1-22. <https://doi.org/10.1090/S0025-5718-1995-1270622-3>
- [5] Helsing, Johan, and Rikard Ojala. "Corner singularities for elliptic problems: Integral equations, graded meshes, quadrature, and compressed inverse preconditioning." *Journal of Computational Physics* 227, no. 20 (2008): 8820-8840. <https://doi.org/10.1016/j.jcp.2008.06.022>
- [6] Bechmann, Andreas. "Perdigão CFD grid study." *Agricultural and Forest Meteorology* 201 (2016): 86-97. <https://doi.org/10.1016/j.agrformet.2014.10.014>
- [7] Rashmi, W., A. F. Ismail, M. Khalid, and Y. Faridah. "CFD studies on natural convection heat transfer of Al₂O₃-water nanofluids." *Heat and Mass Transfer* 47 (2011): 1301-1310. <https://doi.org/10.1007/s00231-011-0792-x>
- [8] Dehbi, Abdel. "A CFD model for particle dispersion in turbulent boundary layer flows." *Nuclear Engineering and Design* 238, no. 3 (2008): 707-715. <https://doi.org/10.1016/j.nucengdes.2007.02.055>
- [9] Koziel, Slawomir, and Leifur Leifsson. "Multi-level CFD-based airfoil shape optimization with automated low-fidelity model selection." *Procedia Computer Science* 18 (2013): 889-898. <https://doi.org/10.1016/j.procs.2013.05.254>
- [10] De Luca, Fabio, Simone Mancini, Salvatore Miranda, and Claudio Pensa. "An extended verification and validation study of CFD simulations for planing hulls." *Journal of Ship Research* 60, no. 02 (2016): 101-118. <https://doi.org/10.5957/jsr.2016.60.2.101>
- [11] Ge, Lixin, and Jun Zhang. "High accuracy iterative solution of convection diffusion equation with boundary layers on nonuniform grids." *Journal of Computational Physics* 171, no. 2 (2001): 560-578. <https://doi.org/10.1006/jcph.2001.6794>
- [12] Ferziger, Joel H., Milovan Perić, and Robert L. Street. "Basic Concepts of Fluid Flow." *Computational Methods for Fluid Dynamics* (2020): 1-21. https://doi.org/10.1007/978-3-319-99693-6_1
- [13] Aswin, V. S., Ashish Awasthi, and C. Anu. "A comparative study of numerical schemes for convection-diffusion equation." *Procedia Engineering* 127 (2015): 621-627. <https://doi.org/10.1016/j.proeng.2015.11.353>
- [14] Michael, E. P. E., J. Dorning, and Rizwan-Uddin. "Studies on nodal integral methods for the convection-diffusion equation." *Nuclear Science and Engineering* 137, no. 3 (2001): 380-399. <https://doi.org/10.13182/NSE137-380>
- [15] Rebhi, Redha, Younes Menni, Giulio Lorenzini, and Hijaz Ahmad. "Forced-Convection Heat Transfer in Solar Collectors and Heat Exchangers: A Review." *Journal of Advanced Research in Applied Sciences and Engineering Technology* 26, no. 3 (2022): 1-15. <https://doi.org/10.37934/araset.26.3.115>
- [16] Al Doori, Wadhah Hussein Abdulrazzaq. "Experiments and Numerical Investigations for Heat Transfer from a Horizontal Plate via Forced Convection Using Pin Fins with Different Hole Numbers." *CFD Letters* 14, no. 9 (2022): 1-14. <https://doi.org/10.37934/cfdl.14.9.114>
- [17] Yüzbaşı, Şuayip, and Murat Karaçayır. "An approximation technique for solutions of singularly perturbed one-dimensional convection-diffusion problem." *International Journal of Numerical Modelling: Electronic Networks, Devices and Fields* 33, no. 1 (2020): e2686. <https://doi.org/10.1002/jnm.2686>
- [18] Bonilla, Jesús, and Santiago Badia. "Maximum-principle preserving space-time isogeometric analysis." *Computer Methods in Applied Mechanics and Engineering* 354 (2019): 422-440. <https://doi.org/10.1016/j.cma.2019.05.042>
- [19] Shen, Chun, Jianbing Li, Yongzhen Li, and Xuesong Wang. "Scattering characteristics of aircraft wake vortex based on the FDTD solution of convection-diffusion equation." In *2019 IEEE International Conference on Computational Electromagnetics (ICCEM)*, pp. 1-3. IEEE, 2019. <https://doi.org/10.1109/COMPTEM.2019.8779128>
- [20] Labbe, O., E. Maglaras, and F. Garnier. "Large-eddy simulation of a turbulent jet and wake vortex interaction." *Computers & Fluids* 36, no. 4 (2007): 772-785. <https://doi.org/10.1016/j.compfluid.2006.06.001>

- [21] Janakiraman, Arun, K. Isaac, Philip Whitefield, and Donald Hagen. "A numerical thermophoretic model for nanoparticle deposition in an aerosol sampling probe." In *17th AIAA Computational Fluid Dynamics Conference*, p. 5351. 2005. <https://doi.org/10.2514/6.2005-5351>
- [22] Fitt, A. D., and M. P. Pope. "De-icing by slot injection." *Acta Mechanica* 147 (2001): 73-86. <https://doi.org/10.1007/BF01182353>
- [23] Abbasbandy, Saeid, Saeed Kazem, Mohammed S. Alhuthali, and Hamed H. Alsulami. "Application of the operational matrix of fractional-order Legendre functions for solving the time-fractional convection-diffusion equation." *Applied Mathematics and Computation* 266 (2015): 31-40. <https://doi.org/10.1016/j.amc.2015.05.003>
- [24] Momani, Shaher. "An algorithm for solving the fractional convection-diffusion equation with nonlinear source term." *Communications in Nonlinear Science and Numerical Simulation* 12, no. 7 (2007): 1283-1290. <https://doi.org/10.1016/j.cnsns.2005.12.007>
- [25] Yedida, Sanyasiraju V. S. S., and Chirala Satyanarayana. "RBF Based Grid-Free Local Scheme With Spatially Variable Optimal Shape Parameter for Steady Convection-Diffusion Equations." *CFD Letters* 4, no. 4 (2012): 151-172.
- [26] Almeida, Alcino Resende, and Renato MacHado Cotta. "Integral transform methodology for convection-diffusion problems in petroleum reservoir engineering." *International Journal of Heat and Mass Transfer* 38, no. 18 (1995): 3359-3367. [https://doi.org/10.1016/0017-9310\(95\)00101-E](https://doi.org/10.1016/0017-9310(95)00101-E)
- [27] Lan, Bin, Haiyan Li, and Jianqiang Dong. "Positivity-preserving scheme without separated method for 2D convection-diffusion equations on polygonal meshes." *Numerical Methods for Partial Differential Equations* 39, no. 3 (2023): 2270-2283. <https://doi.org/10.1002/num.22966>
- [28] Mohammadi, Reza. "Exponential B-Spline Solution of Convection-Diffusion Equations." *Applied Mathematics* 4 (2013): 933-944. <https://doi.org/10.4236/am.2013.46129>
- [29] Shan, Xiaowen. "Simulation of Rayleigh-Bénard convection using a lattice Boltzmann method." *Physical Review E* 55, no. 3 (1997): 2780. <https://doi.org/10.1103/PhysRevE.55.2780>
- [30] Wu, Shuonan, and Jinchao Xu. "Simplex-averaged finite element methods for H (grad), H (curl), and H (div) convection-diffusion problems." *SIAM Journal on Numerical Analysis* 58, no. 1 (2020): 884-906. <https://doi.org/10.1137/18M1227196>
- [31] Chertock, Alina, Charles R. Doering, Eugene Kashdan, and Alexander Kurganov. "A fast explicit operator splitting method for passive scalar advection." *Journal of Scientific Computing* 45 (2010): 200-214. <https://doi.org/10.1007/s10915-010-9381-2>
- [32] Anderson, John D. *Computational fluid dynamics: the basics with applications*. McGraw-Hill, 1995.
- [33] Abdullah, Aslam. "Comparative Study of Uniform and Graded Meshes for Solving Convection-Diffusion Equation with Quadratic Source." *Progress in Aerospace and Aviation Technology* 2, no. 1 (2022): 1-9. <https://doi.org/10.30880/paat.2022.02.01.001>